

Characterization of a Serine/Threonine Kinase Involved in Virulence of *Staphylococcus aureus*[∇]

Michel Débarbouillé,^{1,2}§ Shaynoor Dramsi,^{1,2}§ Olivier Dussurget,^{3,4,5} Marie-Anne Nahori,^{3,4,5}
Elisabeth Vaganay,⁶ Grégory Jouvion,⁷ Alain Cozzone,⁶
Tarek Msadek,^{1,2*} and Bertrand Duclos⁶

Institut Pasteur, Unité de Biologie des Bactéries Pathogènes à Gram Positif,¹ and CNRS URA 2172,² 25 rue du Docteur Roux—75724 Paris Cedex 15, France; Institut Pasteur, Unité des Interactions Bactéries-Cellules,³ Inserm U604,⁴ and INRA USC2020,⁵ 25 rue du Docteur Roux—75724 Paris Cedex 15, France; Unité Mixte de Recherche 5086—CNRS/Université de Lyon, Institut de Biologie et Chimie des Protéines, Lyon, France⁶; and Institut Pasteur, Unité de Recherche et d'Expertise Histotechnologie et Pathologie,⁷ 25 rue du Docteur Roux, 75724 Paris Cedex 15, France

Received 23 December 2008/Accepted 6 April 2009

***Staphylococcus aureus* is a common human cutaneous and nasal commensal and a major life-threatening pathogen. Adaptation to the different environments encountered inside and outside the host is a crucial requirement for survival and colonization. We identified and characterized a eukaryotic-like serine/threonine kinase with three predicted extracellular PASTA domains (SA1063, or Stk1) and its associated phosphatase (SA1062, or Stp1) in *S. aureus*. Biochemical analyses revealed that Stk1 displays autokinase activity on threonine and serine residues and is localized to the membrane. Stp1 is a cytoplasmic protein with manganese-dependent phosphatase activity toward phosphorylated Stk1. In-frame deletions of the *stk1* and *stp1* genes were constructed in *S. aureus* strain 8325-4. Phenotypic analyses of the mutants revealed reduced growth of the *stk1* mutant in RPMI 1640 defined medium that was restored when adenine was added to the medium. Furthermore, the *stk1* mutant displayed increased resistance to Triton X-100 and to fosfomycin, suggesting modifications in cell wall metabolism. The *stk1* mutant was tested for virulence in a mouse pyelonephritis model and found to be strongly reduced for survival in the kidneys (approximately 2-log-unit decrease) compared to the parental strain. Renal histopathological analyses showed severe inflammatory lesions in mice infected with the parental *S. aureus* SH1000 strain, whereas the Δ *stk1* mutant led to only minimal renal lesions. These results confirm the important role of Stk1 for full expression of *S. aureus* pathogenesis and suggest that phosphorylation levels controlled by *stk1* are essential in controlling bacterial survival within the host.**

Protein phosphorylation has been evolutionarily conserved from *Escherichia coli* to *Homo sapiens* and plays a role in a multitude of cellular processes, including proliferation, differentiation, and development. Protein phosphorylation usually results in a functional change of the target protein by modifying enzyme activity, cellular location, or association with other biomolecules (proteins, DNA, or RNA). Phosphorylation/dephosphorylation of serine, threonine, or tyrosine by the respective kinases and phosphatases is used to control many important cellular processes in eukaryotes. In prokaryotes, signal transduction often involves two-component systems, which are composed of a histidine kinase sensing module and its cognate transcriptional regulator. Analysis of the *Staphylococcus aureus* N315 genome sequence predicted 17 potential two-component systems in *S. aureus*, only one of which, WalK/WalR, is known to be essential for bacterial viability (12).

An increasing number of reports describe the existence of eukaryotic-type serine/threonine kinases and phosphatases in prokaryotes. Genes encoding these kinases and phosphatases are often linked and have been identified in soil bacteria, such

as *Myxococcus* spp. (31, 32), *Streptomyces* spp. (39), *Corynebacterium glutamicum* (16), and *Bacillus* spp. (30), as well as in bacterial pathogens, such as *Mycobacterium tuberculosis* (18, 50), *Streptococcus agalactiae* (41), *Streptococcus pneumoniae* (14, 35, 45), *Streptococcus pyogenes* (21), *Streptococcus mutans* (20), *Listeria monocytogenes* (1, 2), and *Enterococcus faecalis* (23).

Global phosphoproteome analyses of *Bacillus subtilis* revealed several potential targets for Ser/Thr kinases involved in processes such as carbohydrate and energy metabolism, transport, stress, and development (15, 27, 29). These results indicate that phosphorylation on serine and threonine residues is more widespread than previously thought. In prokaryotes, many Ser/Thr kinases have now been characterized and shown to regulate various cellular functions, such as developmental processes (30, 33), secondary metabolism (49), stress response (34), biofilm formation (20), antibiotic resistance (23), virulence (8), cell wall biogenesis, cell division, and central metabolism (50). However, a detailed understanding of their mechanisms of action, as well as their specific substrates and precise roles, remains largely elusive. Only a few substrates of specific Ser/Thr kinases and phosphatases have been identified so far, e.g., *B. subtilis* elongation factor EF-G (17) and *S. agalactiae* inorganic pyrophosphatase PpaC (41). Several mycobacterial Stk1 substrates have been identified, including transcription regulators and enzymes of the fatty acid synthase II complex (50). In *L. monocytogenes*, Stp plays a role in virulence, and two

* Corresponding author. Mailing address: Institut Pasteur, Unité de Biologie des Bactéries Pathogènes à Gram Positif, 25 rue du Docteur Roux—75724 Paris Cedex 15, France. Phone: (33) 1 45 68 88 09. Fax: (33) 1 45 68 89 38. E-mail: tmsadek@pasteur.fr.

§ M.D. and S.D. contributed equally to this work.

[∇] Published ahead of print on 24 April 2009.

TABLE 1. *S. aureus* strains and plasmids used in this study

Strain or plasmid	Genotype or description	Source or reference
Strains		
RN4220	Restriction-deficient transformation recipient	Laboratory stock
8325-4	Reference strain <i>rsbU</i> mutant cured of known prophages	38
SH1000	8325-4 <i>rsbU</i> ⁺	19
N315	Methicillin-resistant strain	24
ST1003	8325-4 <i>stp1</i>	This work
ST1004	8325-4 <i>stk1</i>	This work
ST1005	SH1000 <i>stk1</i>	This work
ST1006	8325-4 pMK4-Pprot	This work
ST1007	8325-4 pC2	This work
ST1008	8325-4 <i>stk1</i> pC2	This work
ST1010	8325-4 <i>stk1</i> pMK4-Pprot	This work
Plasmids		
pMAD	pE194 derivative with a thermosensitive origin of replication for deletion replacement of genes in gram-positive bacteria	3
pMK4-Pprot	pMK4 derivative with a constitutive promoter	1
pET15b	<i>E. coli</i> expression vector	Novagen
pC2	pMK4-Pprot derivative carrying the <i>stk1</i> gene with an HA tag	This work
pET-Stk1	pET15b derivative for Stk1 overproduction	This work
pET-Stp1	pET15b derivative for Stp1 overproduction	This work

substrates were identified: the elongation factor EF-Tu and Sod, the manganese-dependent superoxide dismutase (1, 2).

S. aureus is a major human pathogen that causes a number of diseases ranging from skin infections to toxic shock syndrome, osteomyelitis, and myocarditis. Recently, a phosphoproteome analysis of *S. aureus* strain N315 identified nine glycolytic enzymes as substrates of the endogenous Ser/Thr kinase(s) (28).

In the present work, we investigate the roles of the Stk1/Stp1 Ser/Thr kinase and phosphatase of *S. aureus*. We demonstrate an autophosphorylation activity for Stk1 and show that the Stk1 kinase can be dephosphorylated by the Mn²⁺-dependent phosphatase Stp1. Interestingly, an *stk1* deletion mutant displayed increased resistance to Triton X-100 and to fosfomycin, suggesting modifications in cell wall metabolism, in agreement with the presence of three potential extracellular PASTA (PBP and serine/threonine kinase-associated) domains. We also show that the *stk1* mutant is strongly impaired for survival in a murine pyelonephritis model, with renal histopathological analyses showing minimal lesions compared to the severe inflammatory lesions and necrosis seen in mice infected with the parental SH1000 strain, indicating that the Stk1 kinase plays a major role in virulence.

MATERIALS AND METHODS

Bacterial strains, plasmids, and growth media. The *S. aureus* strains used in this study are listed in Table 1. *E. coli* K-12 strain DH5 α [λ - δ 80dlacZ Δ M15 Δ (*lacZYA-argF*)U169 *recA1 endA1 hsdR17*(r_K⁻ m_K⁻) *supE44 thi-1 gyrA relA1*] (Invitrogen) was used for cloning experiments. *E. coli* BL21 λ DE3 was used for expression of recombinant proteins (47). The plasmid vector pET15 was purchased from Novagen. The pMAD shuttle vector was used for gene replacement (3).

S. aureus was cultured in Trypticase soy broth (TSB) or agar (TSA) and *E. coli* in Luria-Bertani medium. Antibiotics were used at the following concentrations: for *E. coli*, 100 μ g/ml ampicillin; for *S. aureus*, 10 μ g/ml chloramphenicol and 1 μ g/ml erythromycin.

General DNA techniques. The oligonucleotides used in this study are shown in Table 2. Standard techniques were used for nucleic acid cloning and restriction analysis (44). Plasmid DNA from *E. coli* was prepared by rapid alkaline lysis using the Midiprep Plasmid Kit (Qiagen). Genomic DNA from *S. aureus* was

prepared using the MasterPure Gram Positive DNA Purification Kit (Epicentre Biotechnologies). PCR amplifications were carried out with *Pwo* polymerase as recommended by the manufacturer (Roche). Amplification products were purified using the QIAquick PCR purification kit (Qiagen), and nucleotide sequencing of plasmid constructs was carried out by Genome Express-Cogenics.

Expression and purification of recombinant proteins. DNA fragments corresponding to the entire coding sequences of *stk1* (SA1063) and *stp1* (SA1062) were produced using genomic DNA of *S. aureus* strain N315 as a template and the following oligonucleotide pairs: for *stk1*, OBDk1/OBDk2, and for *stp1*, OBDp1/OBDp2. The amplified DNA fragments were digested with NdeI and BamHI and cloned into pET15b. The resulting plasmids, pET-Stk1 and pET-Stp1, were introduced into *E. coli* strain BL21 λ DE3 for protein expression. The six-His-Stk1 and six-His-Stp1 recombinant proteins were purified under native conditions by affinity chromatography on Zn²⁺ columns according to the manufacturer's recommendations (Novagen). Protein purity was checked by sodium dodecyl sulfate-polyacrylamide gel electrophoresis (SDS-PAGE), and protein concentrations were determined using the Coomassie Plus Protein Assay (Pierce).

In vitro phosphorylation assay. In vitro phosphorylation of about 2 μ g of purified six-His-Stk1 protein was performed for 20 min at 37°C in 20 μ l of a buffer containing 25 mM Tris-HCl (pH 7.0), 1 mM dithiothreitol, 1 mM EDTA, 5 mM MnCl₂, and 200 μ Ci [γ -³²P]ATP/ml. In some assays, MnCl₂ was replaced with CaCl₂ or ZnCl₂. In each case, the reaction was stopped by the addition of an equal volume of 2 \times sample buffer (25).

Phosphatase assay. Phosphatase activity was monitored at 37°C by using a continuous method based on the detection of *p*-nitrophenol formed from *p*-nitrophenyl phosphate (*p*NPP). Rates of dephosphorylation were determined by measuring absorbance at 405 nm in a reaction buffer containing Tris-HCl, pH 7.5, 0.1% β -mercaptoethanol, and *p*NPP at concentrations varying from 0.5 to 40 mM. The amounts of *p*-nitrophenol released were determined using a range standard established under the same conditions used in the assay.

Stp1 dephosphorylation assay. In vitro phosphorylation of about 0.5 μ g of purified Stk1 protein was performed as described above. After 10 min of incubation, a dephosphorylation assay of Stk1 was carried out with 0.1 μ g of purified Stp1 at 37°C for 2 to 30 min in 30 μ l of a buffer consisting of 100 mM sodium citrate (pH 6.5) and 1 mM EDTA. The reaction was stopped by the addition of an equal volume of 2 \times sample buffer, and the mixture was heated at 100°C for 5 min. The Stk1 protein was separated by gel electrophoresis, treated with TCA, and analyzed by autoradiography.

Phosphoamino acid content analysis. Determination of phosphoresidues was carried out using two-dimensional migration. After phosphorylation, proteins were separated by SDS-PAGE and transferred onto nylon membranes as previously described (13). The radioactive spot was cut out of the membrane and hydrolyzed by 6 M HCl for 1 h at 110°C. The acid-stable phosphoamino acids thus liberated were separated by electrophoresis in the first dimension at pH 1.9

TABLE 2. Oligonucleotides used in this study

Name	Sequence	Description
OMD208	GAAGAATTCGAATGAAGATGCGGGTGG	<i>stk1</i> deletion
OMD224	CTCCTCGAGTATCATACTTTATCACCTCA	<i>stk1</i> deletion
OMD227	CTCCTCGAGGATATTTAAATATAAATTGAAG	<i>stk1</i> deletion
OMD228	GGAGGATCCGTCAGCTGGCCAAGCTTCTA	<i>stk1</i> deletion
OMD237	GAAGAATTCATAATGGGTATCGGTGAACC	<i>stp1</i> deletion
OMD238	CTCCTCGAGTAGCATTGTCTTTACCTCGT	<i>stp1</i> deletion/RT-PCR
OMD239	CTCCTCGAGGGTGATAAAGTATGATAGGTA	<i>stp1</i> deletion
OMD240	GGAGGATCCATCCGTTGCCACCTTTTGC	<i>stp1</i> deletion
OMD212	GCAAATGTCGGTGATTCTAGACCTATG	RT-PCR
OMD225	CTCCTCGAGGCCACCGCCCAAGCTTATC	RT-PCR
OMD263	GACGGTTCAACTGAAAAAGGTAGTTTCGAC	RT-PCR
OMD264	CGCCATTAACGTCTACTTGATATACCCAC	RT-PCR
OMD289	CCTGTCAACCATGTTCCAGAAAG	RT-PCR
OMD295	CAACATCCGATAACTGGAGAGTTGGTC	RT-PCR
OMD296	CGCTCGAAATTTTGTGACCTTGTTCAAC	RT-PCR
OMD298	CGTGGATTATCACCATGGCCAGTTGC	RT-PCR
OMD301	TGTCATAACACGTTTACGTCCAACAGGTCG	RT-PCR
OMD305	CGGTATCCCTTTTACAGAACGTGCGGACC	RT-PCR
OMD314	AGAAGATCTGTGCGGACCGTATTTTAACAG	RT-PCR
OMD331	CAAAAAGCCCTTGATGCTACAGAAGAGCGC	RT-PCR
OMD332	GTATGTGTAACGACACAAGTAGGTTGTCG	RT-PCR
OMD337	GGAGGATCCATACTCGCGGCTATTGAAGGT	<i>stk1</i> complementation
OMD339	TGCGGTCGACTTAGGCGTAGTCGGGGACGTTAGGGGTA AATATCATCATAGCTGACTTC	<i>stk1</i> complementation HA tag
OBdk1	GGAATTCATATGATAGGTAAAATAATAAATGAAC	Stk1 overproduction
OBdk2	CGCGGATCCTTATACATCATCATAGCTGAC	Stk1 overproduction
OBdp1	GGAATTCATATGGCAATTACAAAATCAATGATT	Stp1 overproduction
OBdp2	CGCGGATCCTTATAGTTCAATTTCTGTTGTT	Stp1 overproduction

(800 V h⁻¹) in 7.8% acetic acid/2.5% formic acid, followed by ascending chromatography in the second dimension in 2-methyl-1-propanol/formic acid/water (8:3:1). After migration, radioactive molecules were detected by autoradiography. The phosphoamino acid standards, phosphoserine, phosphothreonine, and phosphotyrosine, were separated in parallel and revealed by ninhydrin staining. The pattern of phosphoamino acids revealed by ninhydrin was compared with that revealed by autoradiography, in order to determine the nature of the phosphoamino acid.

***stp1* and *stk1* mutant construction.** In-frame deletions in *stp1* and *stk1* were constructed as follows. For each gene inactivation, the upstream and downstream PCR-generated DNA fragments (oligonucleotide pairs OMD237-OMD228 and OMD239-OMD240 for *stp1* and OMD208-OMD224 and OMD227-OMD228 for *stk1*) were digested with XhoI and then ligated using T4 DNA ligase (Biolabs). The ligation product was reamplified using the external primers, purified on an agarose gel using the QIAquick Extraction Kit (Qiagen), digested with the appropriate enzymes (EcoRI and BamHI), and cloned in the thermosensitive shuttle plasmid pMAD (3). Electroporation of *S. aureus* strains and allelic exchange were performed as previously described (3). In-frame deletion mutants were confirmed by PCR and sequence analysis.

Site-directed mutagenesis. Site-directed mutagenesis was carried out using the Transformer Site-Directed Mutagenesis Kit from Clontech as recommended by the manufacturer. This procedure was applied directly to the pET-Stk1 construct. The oligonucleotide primers used for mutagenesis were as follows: K39G, 5'-CAT TAAAGTTGCAATTGCGGCGATTTTATAC-3', and an EcoRI restriction site-eliminating oligonucleotide, 5'-GTTATATCCCGCCGAATTCACCATCAAAAC-3'. The presence of the mutation was verified by DNA sequencing.

Complementation with *stk1*-HA. The entire coding sequence of *stk1* containing an in-frame hemagglutinin (HA) tag at the 3' end (*stk1*-HA) was amplified by PCR from 8325-4 genomic DNA using primers OMD337 and OMD339. After digestion with the appropriate enzymes (SalI and BamHI), the PCR product was cloned into the shuttle vector pMK4-Pprot (1). The construction was verified by sequencing the insert. The resulting plasmid, pC2, was introduced into both the wild-type *S. aureus* strain 8325-4 and the isogenic Δ *stk1* strain by electroporation, giving rise to strains ST1007 and ST1008, respectively.

RNA isolation and cDNA synthesis. Bacteria were grown in TSB (20 ml) to an optical density at 600 nm (OD₆₀₀) of ~0.8. The bacteria were pelleted and immediately frozen at -20°C. RNA extractions were then performed as previously described (6), followed by DNase I treatment with the Turbo-DNA-free

reagent (Ambion, Austin, TX) in order to eliminate residual contaminating genomic DNA. cDNA synthesis was performed as previously described (12).

Bacterial fractionation and immunoblotting. *S. aureus* strain ST1007 was grown to exponential phase in TSB (50 ml), to an OD₆₀₀ of 0.8, and harvested. The supernatant was filtered (0.22 µm) and precipitated with 10% TCA (Sigma). The cell pellet was resuspended in 500 µl of digestion buffer (150 mM NaCl, 20 mM MgCl₂, 30% raffinose) containing 0.5 µg ml⁻¹ lysozyme and lysostaphin. The mixture was incubated at 37°C for 30 min until at least 95% of the cells were protoplasted with no detectable lysis seen by phase-contrast microscopy. The protoplasts were pelleted and resuspended in protoplast lysis buffer (100 mM Tris-HCl, pH 7.5, 100 mM NaCl, 10 mM MgCl₂) for 15 min at 4°C and disrupted by multiple freeze-thaw cycles. The lysed bacteria were then centrifuged (15 min; 20,000 × g). The pellet (membrane fraction) was resuspended in 500 µl of PBS. The protein concentrations of the supernatant, cell wall, membrane, and cytosolic fractions were determined using the bicinchoninic acid protein assay (Pierce). For analysis of Stk1 production, equivalent amounts of all fractions, representing approximately 1 ml of bacterial culture, were analyzed by immunoblotting. The proteins were boiled in Laemmli sample buffer, separated on an 8% SDS-PAGE gel, and transferred to a nitrocellulose membrane. HA-tagged Stk1 was detected using a monoclonal antibody directed against the HA tag (3F9; Roche), horseradish peroxidase-coupled anti-mouse secondary antibodies (Zymed), and the Western blot Pico chemiluminescence kit (Pierce).

Zymograms. Fifty-milliliter cultures were grown in TSB at 37°C with aeration to an OD₆₀₀ of approximately 1, and total protein extracts were prepared by disrupting the cells with a FastPrep cell disintegrator (Bio 101) using the FastPrep FastProtein Blue Protocol (the FastPrep instrument was set at a speed of 6.5 for 30 s). Protein concentrations were determined using the bicinchoninic acid protein assay (Pierce). Equivalent amounts of total protein extracts were subjected to SDS-PAGE with heat-inactivated staphylococcal cells (equivalent to an OD₆₀₀ of 10) as a substrate in the separation gel (12% acrylamide). Following electrophoresis, the gel was washed in water to remove the SDS and to allow protein refolding by incubation in phosphate buffer (0.1 M NaPO₄; pH 7) at 37°C. Protein bands with bacteriolytic activities were detected as clear zones in the opaque gel.

Animal experiments and histopathological analyses. Eight-week-old female CD1 mice (Janvier) were intravenously inoculated with the *S. aureus* parental strain and isogenic mutants. Groups of six mice were infected with 10⁸ CFU per mouse in 0.2 ml. The animals were sacrificed 7 days postinoculation, and the

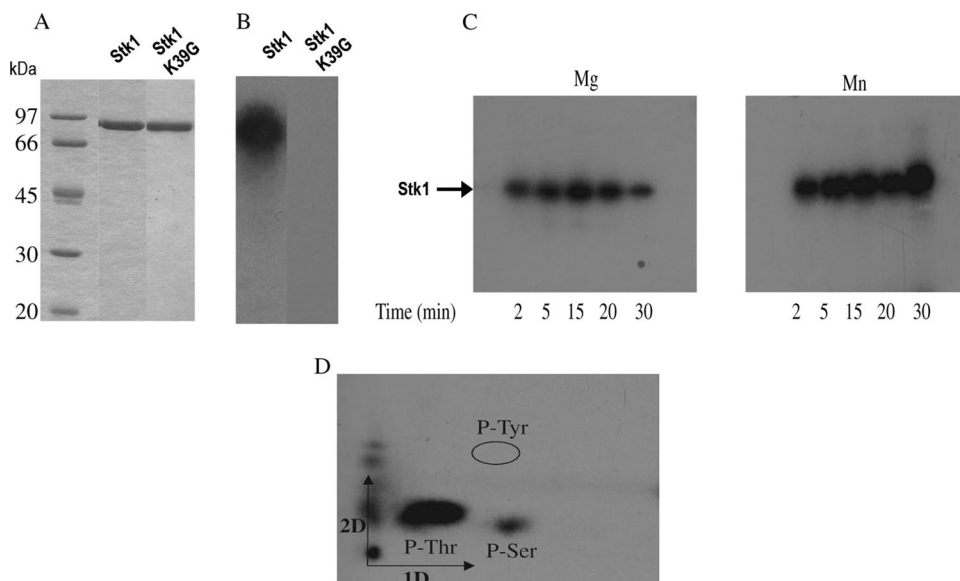


FIG. 1. Biochemical properties of recombinant Stk1. (A) SDS-PAGE analysis of purified Stk1 (lane 2) and Stk1 mutant K39G (lane 3) after staining them with Coomassie blue. Molecular mass standards are indicated on the left (lane 1). (B) Autophosphorylation of Stk1 (lane 1) and mutant K39G (lane 2) in the presence of radioactive $[\gamma\text{-}^{32}\text{P}]\text{ATP}$. (C) Effects of cations on Stk1 activity in vitro. Autophosphorylation of purified Stk1 incubated in the presence of 5 mM manganese (Mn^{2+}) or magnesium (Mg^{2+}) for the indicated times. (D) Two-dimensional analysis of phosphorylated amino acids in Stk1. The acid-stable phosphoamino acids from $\gamma\text{-}^{32}\text{P}$ -labeled Stk1 were separated by electrophoresis in the first dimension (1D), followed by ascending chromatography in the second dimension (2D). P-Tyr, phosphotyrosine; P-Ser, phosphoserine; P-Thr, phosphothreonine.

kidneys were removed and homogenized for determination of the number of bacterial CFU per kidney following dilution and plating on TSA plates. For blood sampling, 10 μl of blood was collected in a heparin-containing syringe from the tail vein of each mouse at days 3, 5, and 7 postinfection. The blood was then directly plated on TSA plates, which were incubated for 24 h at 37°C before colonies were counted.

For histological observations, groups of three mice were infected with 2×10^7 CFU per mouse in 0.2 ml. The animals were sacrificed 7 days postinoculation, and the kidneys were removed and immediately fixed in 4% neutral buffered formalin for the histopathological analysis. After 48 h of fixation, the kidney was longitudinally sectioned through the hilus in order to obtain the renal cortex, medulla, crest, and pelvis on the same section. These samples were embedded in paraffin, and 5- μm sections were cut and stained with hematoxylin and eosin.

RESULTS

Identification of *stk1* and *stp1*. Analysis of the *S. aureus* N315 genome sequence revealed the existence of two adjacent genes, SA1062 and SA1063, encoding proteins sharing similarity with eukaryotic Ser/Thr phosphatases and Ser/Thr kinases, respectively. SA1062 (designated *stp1*) encodes a 247-amino-acid protein displaying 42% identity with PrpC of *B. subtilis* (36), 39% identity with Stp of *L. monocytogenes* (1), 38% identity with Stp1 of *S. agalactiae* (41), and 22% identity with PP2C of *H. sapiens*. These proteins belong to the PPM family, whose founding member is the eukaryotic PP2C. The Stp1 sequence shares 14% amino acid sequence identity with the PP2C-like phosphatase from *H. sapiens* (4). All the motifs required for phosphatase activity, in particular the positions of residues involved in metal binding, such as the aspartate residue, are conserved between Stp1 and PP2C (9). SA1063 (referred to henceforth as *stk1*) encodes a 664-amino-acid protein with the following characteristic features: an amino-terminal domain homologous to the catalytic domain of Ser/Thr kinases (amino

acids [aa] 10 to 268), followed by a transmembrane segment (aa 350 to 372) and three PASTA domains (aa 373 to 440, 441 to 509, and 510 to 575). The important regions in the catalytic domains of STKs are conserved in Stk1, i.e., an ATP-binding site (aa 16 to 39) and a conserved aspartic residue (D_{126}), which is crucial for the catalytic activity of the enzyme. The PASTA domain has also been found in penicillin binding proteins (PBPs), which are involved in cell wall biosynthesis. In PknB, one of several Ser/Thr kinases in *M. tuberculosis*, the four PASTA domains form the extracellular part of the protein and may represent the signal-binding sensor domain (52).

Stk1 displays autokinase activity. The *stk1* gene was amplified and cloned into the expression vector pET15b to allow the synthesis of a recombinant protein with an amino-terminal histidyl tag at the N terminus. The six-His-Stk1 protein was produced following IPTG (isopropyl- β -D-thiogalactopyranoside) induction, and a band of about 75 kDa, consistent with the theoretical molecular mass of the recombinant protein, was purified to homogeneity in a single step using immobilized Zn^{2+} affinity chromatography (Fig. 1A). We included as a negative control the recombinant Stk1 mutant K39G, which is unable to autophosphorylate (B. Duclos, unpublished data). The protein was then assayed for phosphorylation in vitro. In a protein kinase assay using $[\gamma\text{-}^{32}\text{P}]\text{ATP}$ as the phosphate donor, recombinant Stk1 was intensively radiolabeled (Fig. 1B), indicating autophosphorylation activity. The intensity of Stk labeling was higher in the presence of manganese than in the presence of magnesium ions (Fig. 1C). To identify the nature of the autophosphorylated residues in Stk1, the $\gamma\text{-}^{32}\text{P}$ -labeled band was hydrolyzed and the liberated amino acids were analyzed using two-dimensional chromatography and autoradiog-

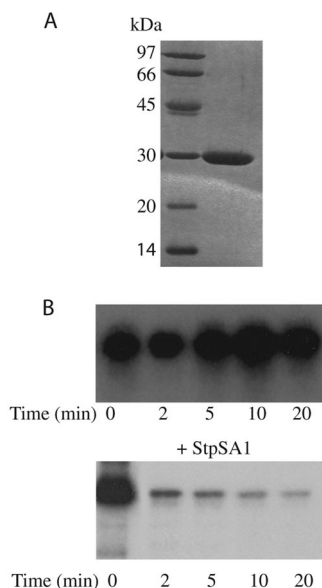


FIG. 2. Biochemical properties of recombinant Stp1. (A) SDS-PAGE analysis of purified Stp1 after being stained with Coomassie blue. Molecular mass standards are indicated on the left. (B) Dephosphorylation of Stk1 by Stp1. Purified Stk1 phosphorylated in vitro with [γ - 32 P]ATP was incubated without (top) or with (bottom) Stp1 for the indicated times. Equal amounts of Stk1 were analyzed by electrophoresis, and radioactivity was revealed by autoradiography.

raphy. Both phosphothreonine and, to a lesser extent, phosphoserine were detected on the corresponding autoradiogram (Fig. 1D), demonstrating that Stk1 is indeed a Ser/Thr protein kinase.

Stp1 is a manganese-dependent phosphatase. The *stp1* gene was amplified and cloned into the pET15b plasmid to allow the synthesis of a recombinant protein with an amino-terminal histidyl tag. The six-His-Stp1 protein was expressed following IPTG induction, and a band of about 33 kDa, consistent with the theoretical molecular mass of the recombinant protein, was purified to homogeneity in a single step using immobilized Zn^{2+} affinity chromatography (Fig. 2A). The phosphatase activity of six-His-Stp1 was first analyzed for its ability to cleave *p*NPP. Hydrolysis of *p*NPP by Stp1 was measured in the presence of various divalent cations: Mn^{2+} , Mg^{2+} , Ca^{2+} , and Zn^{2+} . We found that the catalytic activity of Stp1 using *p*NPP as a substrate was observed only in the presence of Mn^{2+} (data not shown). Optimal phosphatase activity was seen at an Mn^{2+} concentration of 5 mM, pH 8.8, at 37°C. This value is close to that reported for orthologous phosphatases (36). Protein phosphorylation is a reversible process, and we therefore determined whether Stp1 could utilize Stk1 as an endogenous substrate and catalyze its dephosphorylation. To test this hypothesis, γ - 32 P-radiolabeled Stk1 was incubated in the presence of Stp1. As shown in Fig. 2B, Stp1 could rapidly and extensively dephosphorylate Stk1 in a time-dependent manner. Analysis of the phosphoamino acids liberated during the reaction showed that serine and threonine residues were dephosphorylated (data not shown). These data provide evidence that phosphorylated Stk1 is an endogenous substrate for Stp1.

***stk1* and *stp1* form an operon in *S. aureus*.** DNA sequence analysis revealed that the last codon of *stp1* overlaps with the

first codon of *stk1* by 1 nucleotide, suggesting that the two genes are cotranscribed and translationally coupled. To demonstrate cotranscription between *stp1* and *stk1*, we performed reverse transcriptase (RT) PCRs using various combinations of primers. The results are summarized in Fig. 3. In all cases, a reaction without RT was also carried out to exclude the presence of contaminating genomic DNA in the RNA preparations. The primer pair OMD212-OMD225, encompassing the 3' end of *stp1* and the 5' end of *stk1*, gave an amplified fragment of the expected size of 460 bp. In addition, an upstream primer, OMD289, hybridizing within the 3' end of the gene upstream from *stp1* (SA1061), also gave an amplified fragment of 990 bp with OMD225. This fragment of 990 bp encompasses the 3' end of SA1061, the entire *stp1* gene, and the 5' end of *stk1*. A similar experiment was carried out using OMD238 (5' end of *stp1*) with either OMD331 or OMD332 (both located in SA1061), giving PCR products of 640 bp and 760 bp, respectively. No PCR product could be detected when an oligonucleotide further upstream (OMD295), located within SA1060, was used. SA1060 and SA1061 (encoding proteins with unknown functions) are separated by only 2 bp. The two genes located immediately upstream from SA1060 and SA1061, SA1058 and SA1059, encode peptidyl deformylase and methionyl tRNA formyl transferase, respectively. Oligonucleotide pairs OMD301-OMD305, OMD298-OMD314, and OMD295-OMD296 were used in similar RT-PCR experiments, giving PCR products of 200 bp, 400 bp, and 250 bp, respectively (Fig. 3 and data not shown). Taken together, these results indicate that *stp1* and *stk1* are the last two genes of a six-gene operon. No PCR products were detected for the intergenic region between *stk1* and the downstream SA1064 gene, indicating that the latter gene is transcribed independently.

Phenotypic analysis of the *stp1* and *stk1* mutants in *S. aureus*. We constructed in-frame deletion mutants in *stp1* and *stk1* in *S. aureus* strain 8325-4 (see Materials and Methods). The two isogenic mutants ST1003 (Δ *stp1*) and ST1004 (Δ *stk1*) displayed similar growth characteristics in TSB compared to the parental strain at 37°C (not shown). Analysis of wild-type and mutant cell morphologies by light and scanning electron microscopy did not reveal any major differences. In contrast to the pleiotropic defects of Ser/Thr kinase mutants in other pathogens (14, 20, 21, 45), only a few phenotypes were observed for the Δ *stk1* mutant. Interestingly, growth curves using the defined RPMI 1640 medium showed reduced growth of the Δ *stk1* mutant compared to the parental wild-type strain (Fig. 4A). Growth of the Δ *stp1* mutant was also reduced in RPMI medium, but to a lesser extent than that observed for the Δ *stk1* mutant (data not shown). Since purine biosynthesis is controlled by a Ser/Thr kinase in *S. agalactiae* (42), we hypothesized that delayed growth in RPMI 1640 medium could be due to the absence of purines. Indeed, supplementing RPMI 1640 medium with 200 μ M adenine relieved the delayed growth of the Δ *stk1* mutant, consistent with a purine biosynthesis defect in the Δ *stk1* mutant (Fig. 4A). This is consistent with the results obtained in the accompanying publication, where a transcriptome analysis of the Δ *stk1* mutant revealed the loss of expression of genes required for purine and pyrimidine biosynthesis, albeit using a different genetic background (10). Given the presence of multiple PASTA domains in Stk1 (see above), we also investigated cell envelope-related phenotypes, such as re-

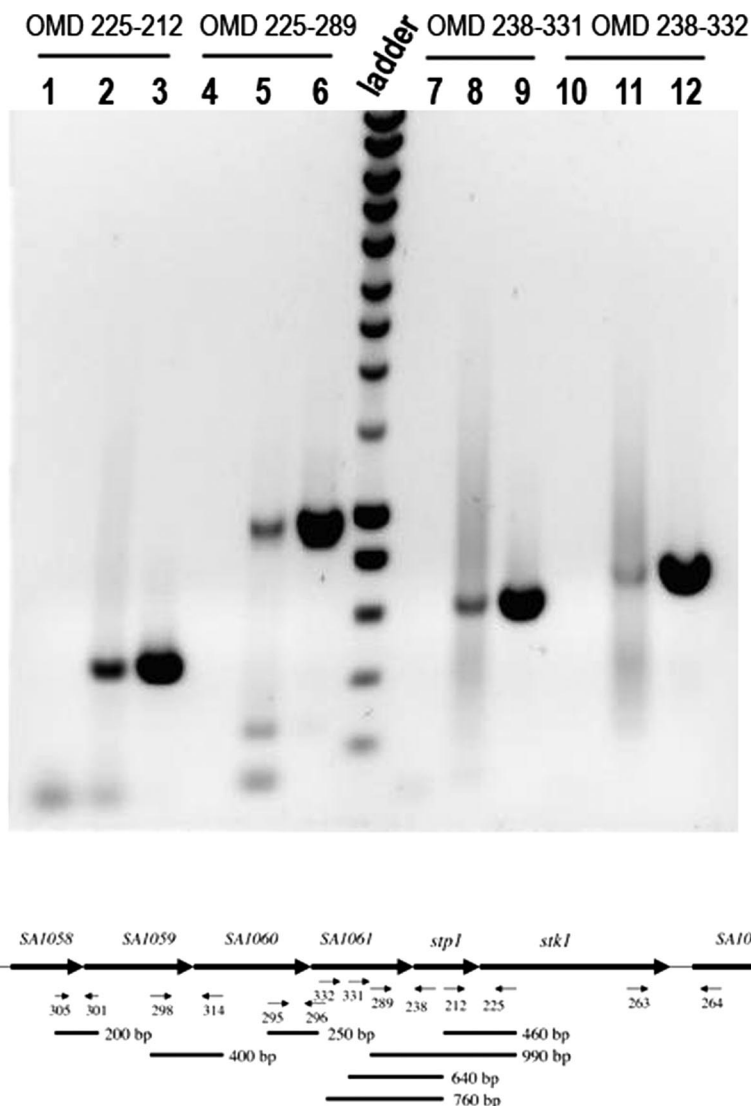
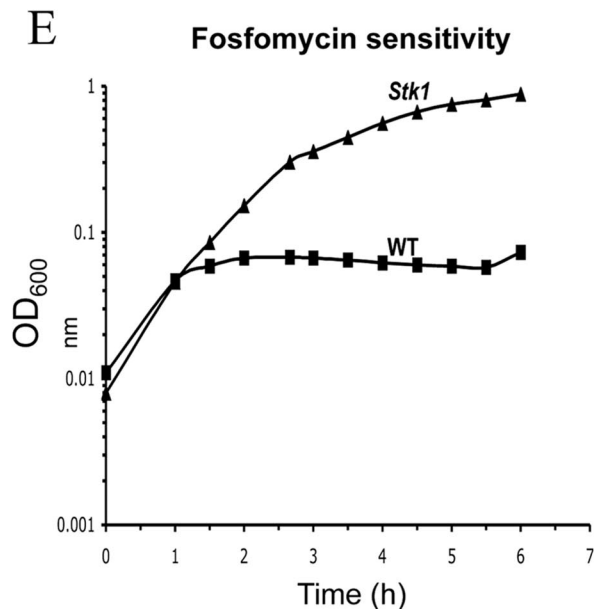
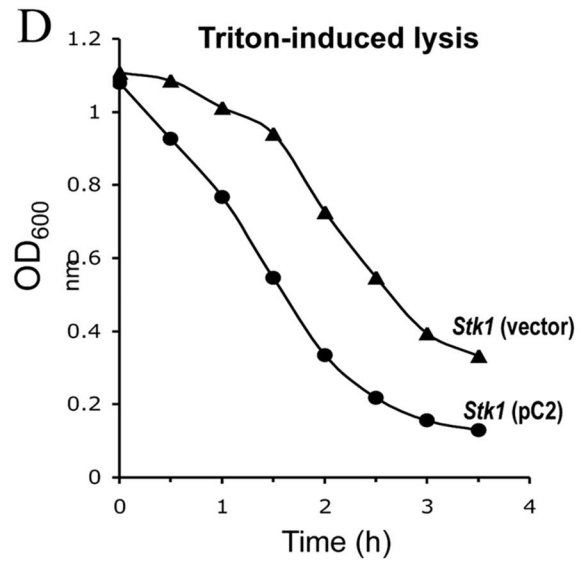
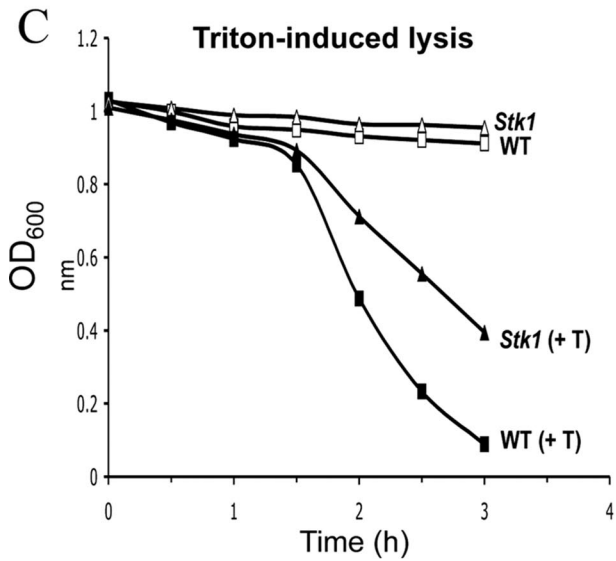
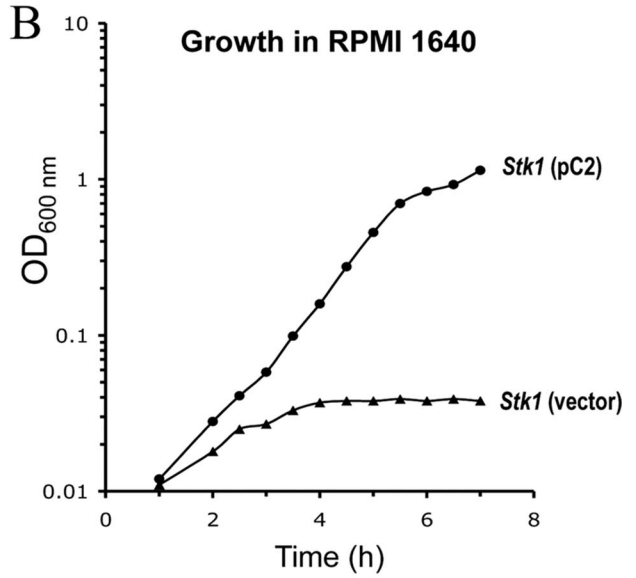
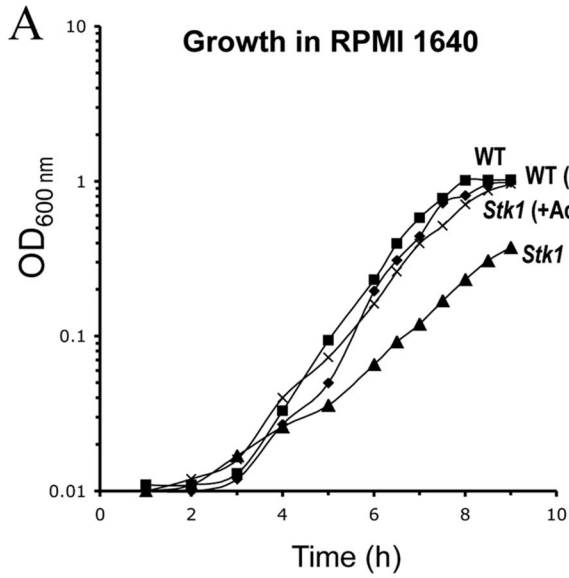


FIG. 3. Physical map of the serine/threonine phosphatase and kinase operon in *S. aureus*. Shown is RT-PCR analysis of *stp1* and *stk1* expression in *S. aureus*. (Top) Cotranscription of *stp1* and *stk1*. DNA PCR products were amplified using the indicated oligonucleotide pairs. Lanes 1, 4, 7, and 10 represent negative controls without RT. Lanes 3, 6, 9, and 12 represent positive controls using chromosomal DNA from strain 8325-4. Lanes 2, 5, 8, and 11 show cotranscriptional analyses of *stp1* and *stk1*. A 1-kb molecular size ladder (Eurogentec) was used. (Bottom) Schematic representation of the *stp1* *stk1* chromosomal region. The thin arrows located below the genes indicate oligonucleotides used in this analysis. Oligonucleotides OMD225, OMD238, OMD264, OMD296, OMD301, and OMD314 were used to synthesize cDNAs from total RNA using RT. The cDNAs were subsequently amplified by PCR, and the black lines represent the amplified fragments.

sistance to antibiotics, autolysis, and sensitivity to lysostaphin and Triton X-100-induced lysis. Resistance to the following antibiotics was tested on Müller-Hinton plates: β -lactams (penicillin, amoxicillin, cefoxitin, cefotaxim, imipenem, moxalactam, and oxacillin), glycopeptides (vancomycin and teicoplanin), aminoglycosides (kanamycin, tobramycin, netilmycin, and gentamicin), and tetracyclines (tetracycline and minocycline), as well as fusidic acid, rifampicin (rifampin), and fosfomycin. The Δ *Stk1* mutant displayed increased resistance to fosfomycin, an antibiotic inhibiting MurA, which catalyzes the first step in peptidoglycan biosynthesis (Fig. 4B). The fosfomycin MICs for the Δ *Stk1* mutant and the parental wild-type strain were determined in liquid cultures: Δ *Stk1*, 64 μ g/ml, and 8325-4, 16 μ g/ml. The Δ *Stk1* mutant was also more resistant to

Triton X-100-induced lysis than the parental strain (Fig. 4C). Complementation of the Δ *Stk1* mutant by introducing a multicopy plasmid carrying the intact *stk1* gene fully restored the growth levels of the Δ *Stk1* mutant in RPMI 1640 medium to those of the parental strain, as well as resistance to Triton X-100-induced lysis (Fig. 4B and D) and sensitivity to fosfomycin (data not shown).

A serine-phosphorylated protein is a target of Stk1. In order to identify possible protein substrates of the Stk1 kinase, we separated total protein extracts from wild-type strain 8325-4 and its isogenic Δ *Stk1* mutant on SDS-PAGE, transferred the proteins to nitrocellulose membranes, and hybridized them with specific anti-phosphoserine and anti-phosphothreonine antibodies, as described in Materials and Methods. Seven



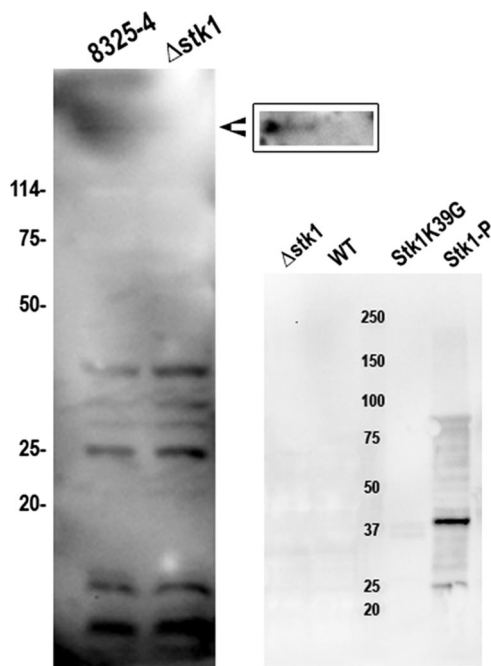


FIG. 5. Phosphorylated proteins in *S. aureus* strain 8325-4 and in the isogenic Δ *stk1* mutant. (Left) Proteins phosphorylated on serine residues were detected by Western blotting using anti-phosphoserine antibodies following 12% SDS-PAGE of total protein extracts from the wild-type (8325-4) and the Δ *stk1* strains harvested during exponential phase. Molecular mass standards (kDa) are indicated on the left. The arrowhead indicates the position of a 120-kDa serine-phosphorylated protein, which is absent in the Δ *stk1* mutant. The inset shows a higher resolution of the missing 120-kDa serine-phosphorylated protein in protein extracts from the Δ *stk1* mutant separated on a 6% SDS-PAGE gel. (Right) Similar analysis with the anti-phosphothreonine antibody. In vitro-phosphorylated Stk1 used as a control showed one strong reactive band with the anti-phosphothreonine antibody. No reactive band was detected in the Stk1 K39G mutant, confirming the specificity of the antibody. WT, wild type.

bands were detected in the wild-type strain with the anti-phosphoserine antibody (Fig. 5, left) and no band with the anti-phosphothreonine antibody (Fig. 5, right). In vitro-phosphorylated Stk1 used as a control showed one strong reactive band with the anti-phosphothreonine antibody. No reactive band was detected in the Stk1 K39G mutant, confirming the specificity of the antibody. Only one of the seven serine-phosphorylated proteins, of approximately 120 kDa, was no longer detected as being phosphorylated in the Δ *stk1* mutant (Fig. 5), suggesting either that these bands correspond to proteins that are phosphorylated on serine residues through the action of other types of kinases, such as PtsK, involved in PTS-depen-

dent sugar transport (43), or RsbW, involved in controlling the activity of sigma B (51), or the possible existence of other, unidentified types of serine kinases in *S. aureus* strain 8325-4. Genome sequence analysis revealed a second atypical serine threonine kinase gene in the first two sequenced strains of *S. aureus*, N315 and Mu50 (SA0077 and SAV0081, respectively). We note, however, that although this second gene is also present in the genomes of strains JH1, JH9, Mu3, and MRSA252, it is absent from the genomes of strains NCTC 8325, 8325-4 (used in this study), COL, MW2, Newman, RF122, USA300, and USA300TCH1516.

Stk1 is essentially membrane bound. Since Stk1-specific antibodies were not available, we used epitope tagging to localize the Stk1 kinase. For that purpose, we inserted the sequence coding for a 9-aa hemagglutinin at the C-terminal end of *stk1* by PCR. The *stk1*-HA gene was amplified using oligonucleotides OMD337 and OMD339.

The PCR fragment was cloned between the BamHI and Sall sites of the pMK4-pProt vector. The resulting plasmid, pC2, was first introduced into *S. aureus* strain RN4220 and then used to transform the wild-type strain 8325-4 and the isogenic Δ *stk1* mutant for complementation. We first analyzed in which bacterial compartment Stk1-HA was located using supernatant, cell wall, membrane, and cytosolic fractions. Stk1 was found to be mostly located in the membrane, but was also present in the cell wall and cytoplasmic fractions (Fig. 6). The cell wall-anchored protein A of *S. aureus* has affinity for the Fc region of immunoglobulins, especially immunoglobulin G. We repeatedly found a band of about 50 kDa in the cell wall and a band of 45 kDa in the supernatant with all the antibodies tested that could correspond to protein A (Fig. 6). As a control, immunoblotting with antibodies against the conserved chaperone DnaK of *E. coli* was done and revealed a band of 75 kDa in *S. aureus*, mostly present in the cytoplasmic fraction, but also in the membrane and cell wall fractions (data not shown). The unexpected presence of DnaK in the cell wall fraction suggests some bacterial lysis may have occurred during preparation of cell wall extracts, and thus, the presence of Stk1 in the cell wall could be an artifact. However, Stk1 is clearly present in the membrane fraction, consistent with the presence of a centrally located transmembrane domain.

Stk1 is required for *S. aureus* virulence in a murine renal-infection model. To investigate the possible involvement of Stp1 and Stk1 in pathogenesis, we used a murine model of hematogenous pyelonephritis. This model utilizes a localized kidney infection from which bacteria can be recovered and quantified. We infected CD1 mice via the lateral tail vein, removed their kidneys at 7 days postinfection, and carried out a quantification of renal bacterial loads, as well as a his-

FIG. 4. Phenotypic analyses of the *stk1* mutant in *S. aureus*. (A) Purine auxotrophy of the *stk1* deletion mutant strain in *S. aureus* strain 8325-4. Cell growth was monitored at OD₆₀₀ in RPMI 1640 synthetic medium at 37°C with or without 200 μM adenine (Ad). ■, wild-type (WT) strain (8325-4) without adenine; ◆, wild-type strain (8325-4) with 200 μM adenine; ▲, strain ST1004 (Δ *stk1*) without adenine; ×, strain ST1004 (Δ *stk1*) with 200 μM adenine. (B) Purine auxotrophy is corrected in the complemented strain. Cell growth was monitored at OD₆₀₀ in RPMI 1640 synthetic medium. ▲, strain ST1010 (Δ *stk1* pMK4-Pprot); ●, strain ST1008 (Δ *stk1* pC2). (C) Triton X-100-induced autolysis of *S. aureus* strains. Shown are strain 8325-4 without (□) or with (■) 0.1% Triton X-100 and strain ST1004 (Δ *stk1*) without (△) or with (▲) 0.1% Triton X-100. (D) Triton X-100-induced autolysis in the complemented strain. ▲, strain ST1010 Δ *stk1* pMK4-Pprot; ●, ST1008 Δ *stk1* pC2. (E) Sensitivity to fosfomycin. Cultures were grown in TSB medium at 37°C in the presence of fosfomycin (9 μg/ml). ■, strain 8325-4; ▲, strain ST1004 (Δ *stk1*).

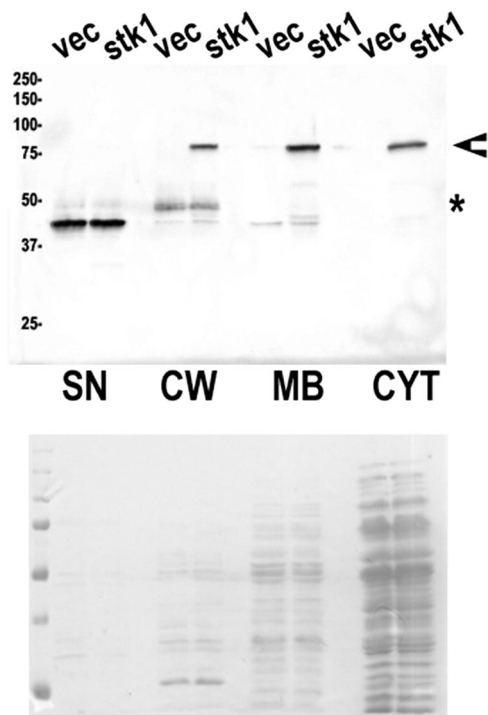


FIG. 6. Subcellular localization of Stk1-HA in *S. aureus*. Exponentially growing cultures of *S. aureus* strain ST1006 (8325-4 carrying the control vector pMK4-Pprot) (vec) or expressing the *stk1*-HA gene (strain ST1007) were fractionated into cytosolic (CYT), membrane (MB), cell wall (CW), and supernatant (SN) compartments and immunoblotted with a commercial anti-HA monoclonal antibody. The equivalent of 1 ml of culture was loaded in each well, and molecular mass standards (kDa) are indicated on the left. Equivalent loading was controlled by staining the nitrocellulose membrane with Ponceau red (bottom) before immunoblotting. The asterisk indicates the presence of the likely protein A band, and the arrowhead indicates the position of the Stk1 band.

topathological analysis of the infected kidney, to investigate the role of Stk1 *in vivo*.

Bacteremia was assessed at various time points during the infection process for the Δ *stp1* and Δ *stk1* mutants and the parental strain, 8325-4. The results showed a 2-log-unit decrease for the Δ *stk1* mutant and 1-log-unit decrease for the Δ *stp1* mutant compared to the wild-type strain, with high variability between mice (data not shown). Since the strain of choice for genetic studies, 8325-4, carries a small deletion in *rsbU*, which encodes a positive regulator of sigma B activity, we checked the effect of the *stk1* deletion in strain SH1000, which is an *rsbU*⁺ derivative of 8325-4 (19). As shown in Fig. 7, the *stk1* deletion in SH1000 clearly reduced bacterial loads in the kidneys. Interestingly, the parental strain, SH1000, gave higher bacterial loads in kidneys than strain 8325-4 (10^8 versus 10^5 CFU, respectively) and less variability between mice. Bacterial loads in the blood were similar between wild-type strains and their isogenic Δ *stk1* mutant during the course of infection, indicating that the reduced kidney colonization of *stk1* deletion mutants was not due to a growth defect or increased sensitivity to immune defenses, such as phagocytosis, antimicrobial peptides, or complement (data not shown). *In vitro* growth curves in murine blood confirmed the absence of growth defects of the Δ *stk1* mutant (data not shown). This result indicates that

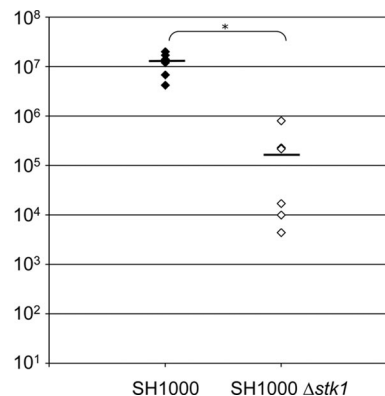


FIG. 7. Role of *S. aureus* Stk1 during infection. Shown is the effect of *stk1* deletion in strain SH1000 on *S. aureus* survival in mice. Bacterial counts of the parental SH1000 and ST1005 (Δ *stk1* mutant) strains were determined in the kidneys of CD1 mice ($n = 6$) 7 days after intravenous injection of 10^8 CFU. Each point is the result for one mouse. The bars represent mean CFU in two kidneys. *, $P < 0.001$ (Student's *t* test).

the virulence defect is not due to a general metabolic defect of the mutant *in vivo*. It also implies that the Δ *stk1* mutant is able to resist phagocytic killing (reactive oxygen species) as well as the wild-type parental strain. To confirm this point, we tested the survival of the *S. aureus* wild-type and Δ *stk1* strains in RAW 264.7 macrophages and did not observe any difference (data not shown). We therefore wondered if Stk1 of *S. aureus* could modulate adhesion and/or invasion of epithelial kidney cells *in vitro* using Madin-Darby canine kidney (MDCK) cells (cell line CCL-34). We did not observe reduced adhesion/invasion for the Δ *stk1* mutant strains compared to the corresponding parental strains (data not shown). Thus, bacterial adhesion to/invasion of host cells, the primary step during kidney infection, is probably not linked to the activity of the serine/threonine kinase in *S. aureus*. However, it remains possible that MDCK cells do not mimic mouse kidney cells.

The renal histopathological analysis revealed significant differences between mice infected with the wild-type SH1000 strain and mice infected with the isogenic Δ *stk1* mutant (Fig. 8). At 7 days postinfection in the kidneys of mice inoculated with the wild-type strain (Fig. 8A to D), we observed multifocal to coalescing inflammatory lesions extending from the renal pelvis to the cortex. These lesions were characterized, in the renal crest, by a severe destruction of the normal tubular organization (Fig. 8A), with collecting tubes either being replaced by an acidophilic and amorphous material containing cell debris (necrosis) and fragmented neutrophils (suppuration) or displaying loss of epithelial cell nuclei associated with a clumping of their cytoplasm but with preservation of the basic outlines of a tubular architecture (ischemic necrosis) (Fig. 8A and B). In the ischemic area, large bacterial colonies were noted (Fig. 8B). Bacteria, associated with neutrophils and cell debris, were also accumulated in the pelvis. These lesions were characteristic of suppurative pyelonephritis. In the cortex, we observed multifocal abscesses measuring up to 1 mm in diameter and displaying a concentric organization (Fig. 8C), characterized from the center to the periphery by (i) an accumulation of fragmented (i.e., karyorrhectic) neutrophils and

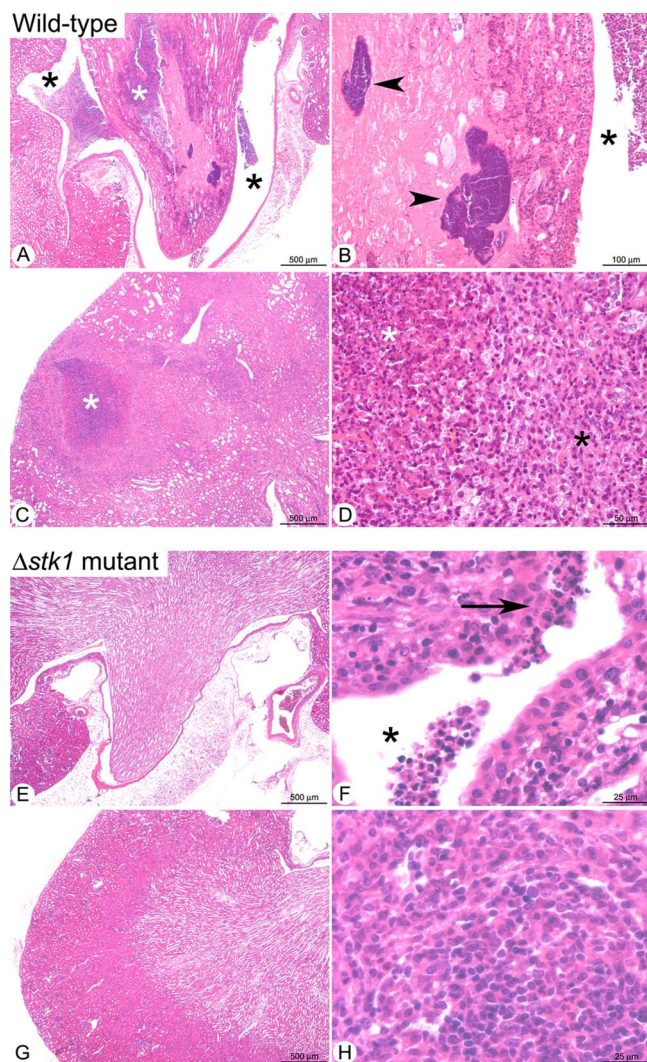


FIG. 8. Histopathological analyses of kidneys in mice infected with either *S. aureus* wild-type strain SH1000 (A to D) or its isogenic Δ *stk1* mutant (E to H). (A) Low magnification of the renal crest (white star) and pelvis (black star), with numerous infiltrates of neutrophils destroying the normal tubular architecture of the tissue. (B) Higher magnification of the renal crest showing bacterial colonies (arrowheads) in a necrotic area (ischemic necrosis). A neutrophilic infiltrate is also observed in the pelvis (black star). (C) Focal abscess in the renal cortex (white star). (D) Higher magnification of the abscess organization, with centrally located fragmented (i.e., karyorrhectic) neutrophils and cell debris (suppuration) (white star) and a peripheral rim of numerous macrophages associated with lymphocytes and plasma cells (black star). (E) Low magnification of the renal crest and pelvis showing no significant histological lesions. (F) Higher magnification of the renal papilli showing a small neutrophilic infiltrate in the pelvis (black star) extending to the overlying epithelium (arrow). (G) Low magnification of the renal cortex with no significant histological lesions. (H) In one mouse, small (less than 150 μ m in diameter) infiltrates of macrophages associated with less numerous lymphocytes and plasma cells were observed in the cortex.

cell debris (suppuration), circled by (ii) a peripheral rim of numerous macrophages and lymphocytes and plasma cells (Fig. 8D). In the residual renal parenchyma, the interstitial connective tissue was diffusely infiltrated by neutrophils and less numerous mononucleated cells, and a high proportion of

tubes in the cortex and the medulla displayed marked dilation of their lumens, filled with cell debris, extracellular proteins, or extravasated erythrocytes (data not shown).

In contrast to these severe lesions, mice infected by the Δ *stk1* mutant displayed only minimal to mild inflammatory lesions (Fig. 8E to H). At low magnification, the medulla appeared morphologically normal (Fig. 8E), but some mice (two of three) displayed small (less than 100- μ m) infiltrates of neutrophils in the pelvis or renal crest (Fig. 8F). The cortices of most mice infected by the Δ *stk1* mutant (two of three) did not display any inflammatory lesions, but in the remaining mouse, small infiltrates (less than 150 μ m in diameter) of macrophages were multifocally observed (Fig. 8H). In contrast to infection with the wild-type strain, bacteria and neutrophils were very rare in the lesions.

DISCUSSION

The availability of an increasing number of bacterial genomes has revealed several eukaryotic-like Ser/Thr protein kinase and phosphatase genes. In this work, we characterized the first genetic locus encoding a eukaryotic-like serine/threonine phosphatase (Stp1) and serine/threonine kinase (Stk1) in *S. aureus*. We showed that histidyl-tagged recombinant Stk1 is a functional protein kinase that autophosphorylates on threonine and serine residues. We also showed that its cognate protein phosphatase, Stp1, specifically dephosphorylates phosphorylated Stk1 in the presence of manganese ions. As previously described in *B. subtilis* (30) and *S. agalactiae* (41), the genes encoding Stp1 and Stk1 were found to be adjacent on the chromosome of *S. aureus*, and we have shown that they are cotranscribed. Together, these results suggest that Stp1 and Stk1 may act as a functional protein pair with antagonistic roles in vivo.

Stk1 belongs to a family of serine/threonine protein kinases, unique to gram-positive bacteria, with a highly conserved intracellular kinase domain and three extracellular PASTA domains. The PASTA domain (PF03793) is found at the C termini of several penicillin-binding proteins and bacterial Ser/Thr kinases (52). This domain was first identified as associated with a high-molecular-weight type II PBP, PBP2X of *S. pneumoniae*, whose structure has been solved (37). The PASTA domain is a small globular fold consisting of three beta-sheets and an alpha-helix that binds the beta-lactam stem, involved in sensing D-alanyl-D-alanine, the PBP transpeptidase substrate. Jones and Dyson (22) compared PASTA sequences found in many bacterial genomes and highlighted their wide divergence, which may reflect the diversity and complexity of peptidoglycan structures. They proposed that these serine/threonine protein kinases might play a key role in peptidoglycan remodeling. Recently, an extracellular domain of the *B. subtilis* PrkC serine/threonine kinase was shown to bind peptidoglycan fragments, thus signaling bacteria to exit dormancy, allowing spore germination (46).

Although we observed that the Δ *stk1* mutant displayed increased resistance to Triton X-100-induced lysis compared to the parental strain, no difference was observed in the autolytic enzyme profile as analyzed by zymograms (data not shown), and scanning electron microscopy did not reveal any morphological differences from the parental strain.

The genetic organization of the *stp1 stk1* locus in *S. aureus* is strikingly similar to that of the *prpC prkC* locus of *B. subtilis*. In *B. subtilis*, *yloQ*, the gene immediately downstream from the Ser/Thr kinase gene *prkC*, was thought to be essential, and the three-dimensional structure of YloQ was recently solved (26). Structural analyses suggest that YloQ is an elongation factor (7). YloQ (also called CpgA) is a GTPase, and analyses of a *yloQ* conditional mutant suggest a role in cell wall biogenesis and morphogenesis. Interestingly, depletion of YloQ in a conditional *yloQ* mutant of *B. subtilis* led to significant sensitivity to fosfomycin (MIC, 8 $\mu\text{g/ml}$ versus 64 $\mu\text{g/ml}$) (5). We observed the opposite effect for the *stk1* deletion mutant strain of *S. aureus* strain 8325-4, which displayed increased resistance to fosfomycin, which exerts its antibacterial effect through inhibition of MurA, catalyzing the first committed step in peptidoglycan synthesis (11). Thus, it is tempting to speculate that Stp1/Stk1 and YloQ are involved in related but still unclear cellular functions, such as peptidoglycan dynamics, cell division, or ribosome function.

The roles of Stk1 and Stp1 in bacterial pathogenesis were studied by deleting the *stp1* and *stk1* genes in *S. aureus* strain 8325-4. Both the Δstp1 and Δstk1 mutants exhibited normal colony morphology and growth in TSB medium. However, using defined RPMI 1640 medium, the *stk1* deletion mutant exhibited an extended lag phase during growth compared to the parental wild-type strain. RPMI 1640 medium is formulated for eukaryotic cell culture and contains amino acids, vitamins, inorganic salts, reduced glutathione, and glucose as the sole carbon source. It was shown that the *stk1*-deficient strain of *S. agalactiae* is unable to sustain purine biosynthesis and is consequently growth arrested (41). We therefore tested the addition of adenine to RPMI 1640 medium and showed that it restored the growth of the 8325-4 Δstk1 mutant to the level of the parental strain (Fig. 4A). Surprisingly, this delayed growth in RPMI 1640 medium was not observed for the Δstk1 mutant in the *rsbU*⁺ genetic background (strain SH1000) (data not shown), suggesting that sigma B may play a role in purine biosynthesis and may modulate the effect of Stk1. It should be noted that RsbU is a PP2C-type serine phosphatase, which could alter the balance of Stk1-phosphorylated proteins, despite the fact that it acts specifically on the phosphorylated form of RsbV (40). In the accompanying paper, Donat et al. (10) performed a transcriptome analysis of the *stk1* deletion mutant and showed that expression levels of purine and pyrimidine biosynthesis genes were significantly lower in the mutant, consistent with the observed growth defect in RPMI 1640.

Over the last few years, extensive work has been performed to demonstrate the important role of bacterial serine/threonine kinases and phosphatases in virulence. Examples include major gram-positive pathogens, such as *S. agalactiae* (41), *E. faecalis* (23), *L. monocytogenes* (1), *S. pyogenes* (21), *S. pneumoniae* (14), and *M. tuberculosis* (50). In *S. agalactiae*, the 50% lethal dose is increased 25-fold for the *stk1* deletion mutant and 100-fold for the double *stk1 stp1* mutant in a rat neonate model. It was hypothesized that this defect could be due to abnormal cell segregation and altered metabolism (41, 42). In *E. faecalis*, PrkC modulates inherent resistance to cell envelope active antimicrobials and intestinal persistence (23). Recently, MgrA, a global regulator in *S. aureus*, was shown to be phosphorylated in a strain overproducing Stk1, leading to in-

creased expression of *norA*, encoding an efflux pump, and concomitant increased resistance to norfloxacin and ciprofloxacin (48). In *S. pneumoniae*, cell wall defects were observed under specific conditions for the *stkP* mutant in vitro (45). The StkP mutant was attenuated for virulence in lungs and blood by approximately 3 log units (14). In all these examples, cell wall defects seemed to be the main cause of attenuation in vivo.

Here, we have shown that the Δstk1 mutant of *S. aureus* exhibited strongly reduced survival in the kidneys of intravenously infected mice. This result was confirmed in two different backgrounds, 8325-4 and SH1000, indicating that Stk1 is required for full virulence of *S. aureus*. Interestingly, bacterial loads in the blood were similar for wild-type and isogenic mutant strains. Histopathological analyses of kidneys showed that mice infected by the wild-type *S. aureus* SH1000 strain displayed marked to severe inflammatory lesions, with numerous intralesional bacteria, in contrast to mice inoculated with the Δstk1 mutant, which had only minimal renal lesions. These results demonstrate that Stk1 is critical for full expression of *S. aureus* pathogenesis.

ACKNOWLEDGMENTS

Work in the group of T. Msadek was supported by research funds from the European Commission (grants from BACELL Health [LSHG-CT-2004-503468], StaphDynamics [LHSM-CT-2006-019064], and BaSysBio [LSHG-CT-2006-037469]), the Centre National de la Recherche Scientifique (CNRS URA 2172), and the Institut Pasteur (GPH no. 9), and work in the group of A. Cozzone was supported by the association Vaincre La Mucoviscidose. G. Jouvion was supported by a Roux Fellowship (Institut Pasteur).

We thank Claire Poyat for help in performing antibiograms; Stéphanie Guadagnini for electron micrographs; Pascale Cossart, in whose laboratory part of this work was carried out; Patrick Trieu-Cuot for helpful discussion; and Sarah Dubrac for critical reading of the manuscript.

REFERENCES

1. Archambaud, C., E. Gouin, J. Pizarro-Cerda, P. Cossart, and O. Dussurget. 2005. Translation elongation factor EF-Tu is a target for Stp, a serine-threonine phosphatase involved in virulence of *Listeria monocytogenes*. *Mol. Microbiol.* **56**:383–396.
2. Archambaud, C., M. A. Nahori, J. Pizarro-Cerda, P. Cossart, and O. Dussurget. 2006. Control of *Listeria* superoxide dismutase by phosphorylation. *J. Biol. Chem.* **281**:31812–31822.
3. Arnaud, M., A. Chastanet, and M. Debarbouille. 2004. New vector for efficient allelic replacement in naturally nontransformable, low-GC-content, gram-positive bacteria. *Appl. Environ. Microbiol.* **70**:6887–6891.
4. Bork, P., N. P. Brown, H. Hegyi, and J. Schultz. 1996. The protein phosphatase 2C (PP2C) superfamily: detection of bacterial homologues. *Protein Sci.* **5**:1421–1425.
5. Campbell, T. L., D. M. Daigle, and E. D. Brown. 2005. Characterization of the *Bacillus subtilis* GTPase YloQ and its role in ribosome function. *Biochem. J.* **389**:843–852.
6. Chastanet, A., M. Prudhomme, J. P. Claverys, and T. Msadek. 2001. Regulation of *Streptococcus pneumoniae* *clp* genes and their role in competence development and stress survival. *J. Bacteriol.* **183**:7295–7307.
7. Cladiere, L., K. Hamze, E. Madec, V. M. Levnikov, A. J. Wilkinson, I. B. Holland, and S. J. Seror. 2006. The GTPase, CpgA(YloQ), a putative translation factor, is implicated in morphogenesis in *Bacillus subtilis*. *Mol. Genet. Genomics* **275**:409–420.
8. Cozzone, A. J. 2005. Role of protein phosphorylation on serine/threonine and tyrosine in the virulence of bacterial pathogens. *J. Mol. Microbiol. Biotechnol.* **9**:198–213.
9. Das, A. K., N. R. Helps, P. T. Cohen, and D. Barford. 1996. Crystal structure of the protein serine/threonine phosphatase 2C at 2.0 Å resolution. *EMBO J.* **15**:6798–6809.
10. Donat, S., K. Streker, T. Schirmeister, and K. Ohlsen. 2009. Transcriptome and functional analysis of the eukaryotic-type Ser/Thr kinase PknB in *Staphylococcus aureus*. *J. Bacteriol.* doi:10.1128/JB0117-09.
11. Du, W., J. R. Brown, D. R. Sylvester, J. Huang, A. F. Chalker, C. Y. So, D. J. Holmes, D. J. Payne, and N. G. Wallis. 2000. Two active forms of UDP-N-

- acetylglucosamine enolpyruvyl transferase in gram-positive bacteria. *J. Bacteriol.* **182**:4146–4152.
12. Dubrac, S., I. G. Boneca, O. Poupel, and T. Msadek. 2007. New insights into the WalK/WalR (YycG/YycF) essential signal transduction pathway reveal a major role in controlling cell wall metabolism and biofilm formation in *Staphylococcus aureus*. *J. Bacteriol.* **189**:8257–8269.
 13. Duclos, B., S. Marcandier, and A. J. Cozzone. 1991. Chemical properties and separation of phosphoamino acids by thin-layer chromatography and/or electrophoresis. *Methods Enzymol.* **201**:10–21.
 14. Echenique, J., A. Kadioglu, S. Romao, P. W. Andrew, and M. C. Trombe. 2004. Protein serine/threonine kinase StkP positively controls virulence and competence in *Streptococcus pneumoniae*. *Infect. Immun.* **72**:2434–2437.
 15. Eymann, C., D. Becher, J. Bernhardt, K. Gronau, A. Klutzny, and M. Hecker. 2007. Dynamics of protein phosphorylation on Ser/Thr/Tyr in *Bacillus subtilis*. *Proteomics* **7**:3509–3526.
 16. Fiuzza, M., M. J. Canova, I. Zanella-Cleon, M. Becchi, A. J. Cozzone, L. M. Mateos, L. Kremer, J. A. Gil, and V. Molle. 2008. From the characterization of the four serine/threonine protein kinases (PknA/B/G/L) of *Corynebacterium glutamicum* toward the role of PknA and PknB in cell division. *J. Biol. Chem.* **283**:18099–18112.
 17. Gaidenko, T. A., T. J. Kim, and C. W. Price. 2002. The PrpC serine-threonine phosphatase and PrkC kinase have opposing physiological roles in stationary-phase *Bacillus subtilis* cells. *J. Bacteriol.* **184**:6109–6114.
 18. Greenstein, A. E., C. Grundner, N. Echols, L. M. Gay, T. N. Lombana, C. A. Mieczkowski, K. E. Pullen, P. Y. Sung, and T. Alber. 2005. Structure/function studies of Ser/Thr and Tyr protein phosphorylation in *Mycobacterium tuberculosis*. *J. Mol. Microbiol. Biotechnol.* **9**:167–181.
 19. Horsburgh, M. J., J. L. Aish, I. J. White, L. Shaw, J. K. Lithgow, and S. J. Foster. 2002. σ^B modulates virulence determinant expression and stress resistance: characterization of a functional *rsbU* strain derived from *Staphylococcus aureus* 8325-4. *J. Bacteriol.* **184**:5457–5467.
 20. Hussain, H., P. Branny, and E. Allan. 2006. A eukaryotic-type serine/threonine kinase is required for biofilm formation, genetic competence, and acid resistance in *Streptococcus mutans*. *J. Bacteriol.* **188**:1628–1632.
 21. Jin, H., and V. Pancholi. 2006. Identification and biochemical characterization of a eukaryotic-type serine/threonine kinase and its cognate phosphatase in *Streptococcus pyogenes*: their biological functions and substrate identification. *J. Mol. Biol.* **357**:1351–1372.
 22. Jones, G., and P. Dyson. 2006. Evolution of transmembrane protein kinases implicated in coordinating remodeling of gram-positive peptidoglycan: inside versus outside. *J. Bacteriol.* **188**:7470–7476.
 23. Kristich, C. J., C. L. Wells, and G. M. Dunny. 2007. A eukaryotic-type Ser/Thr kinase in *Enterococcus faecalis* mediates antimicrobial resistance and intestinal persistence. *Proc. Natl. Acad. Sci. USA* **104**:3508–3513.
 24. Kuroda, M., T. Ohta, I. Uchiyama, T. Baba, H. Yuzawa, I. Kobayashi, L. Cui, A. Oguchi, K. Aoki, Y. Nagai, J. Lian, T. Ito, M. Kanamori, H. Matsumaru, A. Maruyama, H. Murakami, A. Hosoyama, Y. Mizutani-Ui, N. K. Takahashi, T. Sawano, R. Inoue, C. Kaito, K. Sekimizu, H. Hirakawa, S. Kuhara, S. Goto, J. Yabuzaki, M. Kanehisa, A. Yamashita, K. Oshima, K. Furuya, C. Yoshino, T. Shiba, M. Hattori, N. Ogasawara, H. Hayashi, and K. Hiramatsu. 2001. Whole genome sequencing of methicillin-resistant *Staphylococcus aureus*. *Lancet* **357**:1225–1240.
 25. Laemmli, U. K. 1970. Cleavage of structural proteins during the assembly of the head of bacteriophage T4. *Nature* **227**:680–685.
 26. Levdikov, V. M., E. V. Blagova, J. A. Brannigan, L. Cladiere, A. A. Antson, M. N. Isupov, S. J. Seror, and A. J. Wilkinson. 2004. The crystal structure of YloQ, a circularly permuted GTPase essential for *Bacillus subtilis* viability. *J. Mol. Biol.* **340**:767–782.
 27. Levine, A., F. Vannier, C. Absalon, L. Kuhn, P. Jackson, E. Scrivener, V. Labas, J. Vinh, P. Courtney, J. Garin, and S. J. Seror. 2006. Analysis of the dynamic *Bacillus subtilis* Ser/Thr/Tyr phosphoproteome implicated in a wide variety of cellular processes. *Proteomics* **6**:2157–2173.
 28. Lomas-Lopez, R., P. Paracuellos, M. Riberty, A. J. Cozzone, and B. Duclos. 2007. Several enzymes of the central metabolism are phosphorylated in *Staphylococcus aureus*. *FEMS Microbiol. Lett.* **272**:35–42.
 29. Macek, B., I. Mijakovic, J. V. Olsen, F. Gnad, C. Kumar, P. R. Jensen, and M. Mann. 2007. The serine/threonine/tyrosine phosphoproteome of the model bacterium *Bacillus subtilis*. *Mol. Cell. Proteomics* **6**:697–707.
 30. Madec, E., A. Laszkiewicz, A. Iwanicki, M. Obuchowski, and S. Seror. 2002. Characterization of a membrane-linked Ser/Thr protein kinase in *Bacillus subtilis*, implicated in developmental processes. *Mol. Microbiol.* **46**:571–586.
 31. Munoz-Dorado, J., S. Inouye, and M. Inouye. 1991. A gene encoding a protein serine/threonine kinase is required for normal development of *M. xanthus*, a gram-negative bacterium. *Cell* **67**:995–1006.
 32. Munoz-Dorado, J., S. Inouye, and M. Inouye. 1990. Nucleoside diphosphate kinase from *Myxococcus xanthus*. II. Biochemical characterization. *J. Biol. Chem.* **265**:2707–2712.
 33. Nariya, H., and S. Inouye. 2005. Identification of a protein Ser/Thr kinase cascade that regulates essential transcriptional activators in *Myxococcus xanthus* development. *Mol. Microbiol.* **58**:367–379.
 34. Neu, J. M., S. V. MacMillan, J. R. Nodwell, and G. D. Wright. 2002. StoPK-1, a serine/threonine protein kinase from the glycopeptide antibiotic producer *Streptomyces toyocaensis* NRRL 15009, affects oxidative stress response. *Mol. Microbiol.* **44**:417–430.
 35. Novakova, L., L. Saskova, P. Pallova, J. Janecek, J. Novotna, A. Ulrych, J. Echenique, M. C. Trombe, and P. Branny. 2005. Characterization of a eukaryotic type serine/threonine protein kinase and protein phosphatase of *Streptococcus pneumoniae* and identification of kinase substrates. *FEBS J.* **272**:1243–1254.
 36. Obuchowski, M., E. Madec, D. Delattre, G. Boel, A. Iwanicki, D. Foulger, and S. J. Seror. 2000. Characterization of PrpC from *Bacillus subtilis*, a member of the PPM phosphatase family. *J. Bacteriol.* **182**:5634–5638.
 37. Pares, S., N. Mouz, Y. Petillot, R. Hakenbeck, and O. Dideberg. 1996. X-ray structure of *Streptococcus pneumoniae* PBP2x, a primary penicillin target enzyme. *Nat. Struct. Biol.* **3**:284–289.
 38. Peng, H. L., R. P. Novick, B. Kreiswirth, J. Kornblum, and P. Schlievert. 1988. Cloning, characterization, and sequencing of an accessory gene regulator (*agr*) in *Staphylococcus aureus*. *J. Bacteriol.* **170**:4365–4372.
 39. Petrickova, K., and M. Petricek. 2003. Eukaryotic-type protein kinases in *Streptomyces coelicolor*: variations on a common theme. *Microbiology* **149**:1609–1621.
 40. Price, C. W. 2002. General stress response, p. 369–384. In A. L. Sonenshein, J. A. Hoch, and R. M. Losick (ed.), *Bacillus subtilis* and its closest relatives: from genes to cells. ASM Press, Washington, DC.
 41. Rajagopal, L., A. Clancy, and C. E. Rubens. 2003. A eukaryotic type serine/threonine kinase and phosphatase in *Streptococcus agalactiae* reversibly phosphorylate an inorganic pyrophosphatase and affect growth, cell segregation, and virulence. *J. Biol. Chem.* **278**:14429–14441.
 42. Rajagopal, L., A. Vo, A. Silvestroni, and C. E. Rubens. 2005. Regulation of purine biosynthesis by a eukaryotic-type kinase in *Streptococcus agalactiae*. *Mol. Microbiol.* **56**:1329–1346.
 43. Reizer, J., C. Hoischen, F. Titgemeyer, C. Rivolta, R. Rabus, J. Stulke, D. Karamata, M. H. Saier, Jr., and W. Hillen. 1998. A novel protein kinase that controls carbon catabolite repression in bacteria. *Mol. Microbiol.* **27**:1157–1169.
 44. Sambrook, J., E. F. Fritsch, and T. Maniatis. 1989. Molecular cloning: a laboratory manual. Cold Spring Harbor Laboratory, Cold Spring Harbor, NY.
 45. Saskova, L., L. Novakova, M. Basler, and P. Branny. 2007. Eukaryotic-type serine/threonine protein kinase StkP is a global regulator of gene expression in *Streptococcus pneumoniae*. *J. Bacteriol.* **189**:4168–4179.
 46. Shah, I. M., M. H. Laaberki, D. L. Popham, and J. Dworkin. 2008. A eukaryotic-like Ser/Thr kinase signals bacteria to exit dormancy in response to peptidoglycan fragments. *Cell* **135**:486–496.
 47. Studier, F. W., and B. A. Moffatt. 1986. Use of bacteriophage T7 RNA polymerase to direct selective high-level expression of cloned genes. *J. Mol. Biol.* **189**:113–130.
 48. Truong-Bolduc, Q. C., Y. Ding, and D. C. Hooper. 2008. Posttranslational modification influences the effects of MgrA on *norA* expression in *Staphylococcus aureus*. *J. Bacteriol.* **190**:7375–7381.
 49. Umeyama, T., P. C. Lee, and S. Horinouchi. 2002. Protein serine/threonine kinases in signal transduction for secondary metabolism and morphogenesis in *Streptomyces*. *Appl. Microbiol. Biotechnol.* **59**:419–425.
 50. Wehenkel, A., M. Bellinzoni, M. Grana, R. Duran, A. Villarino, P. Fernandez, G. Andre-Leroux, P. England, H. Takiff, C. Cervenansky, S. T. Cole, and P. M. Alzari. 2008. Mycobacterial Ser/Thr protein kinases and phosphatases: physiological roles and therapeutic potential. *Biochim. Biophys. Acta* **1784**:193–202.
 51. Yang, X., C. M. Kang, M. S. Brody, and C. W. Price. 1996. Opposing pairs of serine protein kinases and phosphatases transmit signals of environmental stress to activate a bacterial transcription factor. *Genes Dev.* **10**:2265–2275.
 52. Yeats, C., R. D. Finn, and A. Bateman. 2002. The PASTA domain: a beta-lactam-binding domain. *Trends Biochem. Sci.* **27**:438.